PROCEEDINGS OF SPIE

SPIEDigitalLibrary.org/conference-proceedings-of-spie

Bismuth silicates: preparation by pulsed laser ablation and photocatalytic activity

Golubovskaya, Aleksandra, Fakhrutdinova, Elena, Svetlichnyi, Valery

Aleksandra G. Golubovskaya, Elena D. Fakhrutdinova, Valery A. Svetlichnyi, "Bismuth silicates: preparation by pulsed laser ablation and photocatalytic activity," Proc. SPIE 12086, XV International Conference on Pulsed Lasers and Laser Applications, 120861Y (2 December 2021); doi: 10.1117/12.2612743

SPIE.

Event: XV International Conference on Pulsed Lasers and Laser Applications, 2021, Tomsk, Russian Federation

Bismuth silicates: preparation by pulsed laser ablation and photocatalytic activity

Aleksandra G. Golubovskaya*, Elena D. Fakhrutdinova, Valery A. Svetlichnyi
Laboratory of Advanced Materials and Technology, Tomsk State University,
634050, Tomsk, Lenin av. 36, Russian Federation

ABSTRACT

Pulsed laser ablation (PLA) in liquid is advanced method for obtaining active nanoparticles in pure solvents without the use of chemical precursors. In this work, an original approach to the synthesis of complex oxides of bismuth and silicon (BSO) is proposed. The initial colloids obtained by PLA (Nd:YAG laser, 1064 nm, 7 ns) of Bi and Si targets in water were mixed and subjected to additional irradiation with the same laser parameters. Laser treatment stimulated the formation of complex oxides. Then the colloids were dried in air and nanopowders obtained were studied by X-ray diffraction (XRD), transmission electron microscopy (TEM) and UV-Vis spectroscopy. The photocatalytic activity of the materials was examined in the Rhodamine B degradation under LED source irradiation (375 nm).

Keywords: pulsed laser ablation, laser treatment, nanoparticles, bismuth silicates, photocatalysis

1. INTRODUCTION

Development of photochemical and photocatalytic technologies plays an important role in environmental pollution control[1-3]. Besides, photocatalytic technology is promising green technology for generating hydrogen as well as for the synthesis of new materials[4,5]. In addition to conventional semiconductor nanoparticles (NPs), such as oxides (TiO_2, ZnO)[6,7] and sulfides[8,9], in recent decades complex oxides, heterostructures and other composite nanomaterials have been widely used as photocatalysts[4,5,10-12]. The development of such materials allows increasing the photocatalyst performances, including controling of the band gap for efficient light absorption and promoting of electron-hole pairs separation.

Recently, bismuth silicates, or complex oxides of bismuth and silico (BSO), and composites based on them have been classified as promising photocatalytic materials[13,14]. These materials have good chemical and optical stability and high photoconductivity. The binary Bi_2O_3–SiO_2 system includes three compounds with different composition and structures: bismuth metasilicate (Bi_2SiO_5), bismuth orthosilicate ($Bi_4Si_3O_{12}$), and bismuth sillenite ($Bi_{12}SiO_{20}$)[15]. Bismuth silicates can be obtained by different methods, including solvothermal and hydrothermal methods[16], sol-gel synthesis[17], the Pechini method[18], and mechanochemical synthesis[14].

One of the promising methods of the NP preparation for catalytic application is pulsed laser ablation (PLA) in a liquid[19-21]. The PLA is distinguished by its simplicity, variability, the absence of chemical precursors, and a number of other advantages that make it possible to produce unique NPs, for example, dark TiO_2[22]. Recent advances in preparation of complex nanostructures by PLA[23] allow using it for BSO synthesis. In[24] we applied laser treatment for fragmentation and modification of the chemically prepared BSO.

In the work, we present a new approach to the preparation of bismuth silicates for photocatalytic applications, combining pulsed laser ablation in water and laser treatment of mixed colloid.

*aleksandra.golubovskaya@mail.ru; phone/fax +7 3822 53-15-91; amtlab.ru

XV International Conference on Pulsed Lasers and Laser Applications, edited by Anton V. Klimkin, Maxim V. Trigub, Victor F. Tarasenko, Proc. of SPIE Vol. 12086, 120861Y · © 2021 SPIE · 0277-786X · doi: 10.1117/12.2612743

2. EXPERIMENTAL

2.1 Synthesis of bismuth silicates

The preparation of bismuth silicates was carried out in two stages. At first, individual colloids were obtained by PLA of bismuth and silicon targets. A detailed procedure of synthesis and experimental setup are presented in[25]. For the ablation, Nd:YAG laser LS2131M-20, LOTIS TII (Belarus) with a wavelength of 1064 nm, pulse duration of 7 nm, 20 Hz pulse frequency and pulse energy up to 150 mJ was used. Bi and Si targets were fixed with tweezers on a motorized positioner and placed in a reactor with distilled water. Laser irradiation was focused on the target surface through the wall side of the reactor using lens with a focal length F=50 mm. In order to avoid the formation of craters on the target surface, system was moved in the XY plane along "snake" trajectory. Ablation lasted for 10-15 minutes for the Bi target, and for 50-70 minutes for the Si target. The Bi and Si particle concentration (determined using target mass detection before and after the ablation) was 0.7 and 0.2 g/L, respectively. The colloid obtained by PLA of Bi was dark brown, and that obtained by PLA of Si was light brown. Then, two colloids obtained were mixed in molar ratios Bi:Si = 2:1, 4:3 and 12:1 corresponding to the stoichiometric composition of metasilicate (Bi_2SiO_5), orthosilicate ($Bi_4Si_3O_{12}$) and bismuth sillenite ($Bi_{12}SiO_{20}$), respectively. One part of the solution after mixing was dried in air at temperature of 60 °C. Another part of the solutions was irradiated by focused laser beam with the same Nd:YAG laser for 3 hours. During irradiation, the mixed colloid was stirred with a magnetic stirrer for its homogeneous irradiation. As a result of the laser treatment, clear light brown solutions were obtained. Irradiated colloids were dried under the same conditions as non-irradiated ones. Powder samples obtained from the non-irradiated colloids were designated as BSO1 (Bi:Si=2:1), BSO2 (Bi:Si=4:3), and BSO3 (Bi:Si=12:1), while samples obtained from the colloids with after additional laser treatment were designated as BSO1_hν, BSO2_hν and BSO3_hν, respectively.

2.2 Sample characterization

The crystal structure of the samples was studied by X-ray diffraction (XRD) using an XRD 6000 diffractometer, Shimadzu (Japan). The phase composition was identified using the PDF4 database. The morphology of nanoparticles was studied by the transmission electron microscopy (TEM) using an electron microscope CM12, Philips (Netherlands). The specific surface area (SSA) was determined by the Brunauer–Emmett–Teller (BET) methods using a TriStar II 3020 surface area and porosity analyzer, Micromeritics (USA). The optical properties of the samples were studied by UV-vis spectroscopy in a diffuse reflection (DR) mode with a spectrophotometer Cary 100 SCAN, Varian (Australia), with an accessory of DRA-CA-30I, Labsphere (USA), in the wavelength range 200-800 nm. MgO was used as a reference standard for measurements.

2.3 Photocatalytic activity test

The photocatalytic activity of the bismuth silicates was estimated in the degradation of the Rhodamine B used as a model dye. The sample in amount of 15 mg and 30 ml of an aqueous solution of Rhodamine B with a concentration 5×10^{-6} mol/l were placed in a cylindrical beaker. Before irradiation, the system was placed in the dark for 1 h to establish sorption equilibrium. Irradiation was carried out using a LED source with the wavelength λ_{max}=375 nm. During the dark stage and photocatalytic experiment the system was stirred by a magnetic stirrer. Rhodamine B photodecomposition was determined using change in the optical density of the absorption spectra at a wavelength of 553 nm (maximum absorption of Rhodamine B). To determine the concentration of dye, an aliquot of solution was taken once an hour and the absorption spectra were registered on spectrophotometer Cary 100 SCAN, Varian (Australia).

3. RESULTS AND DISCUSSION

3.1 Structure and properties of samples

Figure 1 presents the XRD patterns of the samples and Table 1 gives their phase composition. In the BSO1 and BSO2 samples only metallic bismuth is detected. This indicates that the colloidal species obtained by PLA of silicon prevent the oxidation of bismuth in mixed colloid. With a decrease in the amount of silicon in the system, in the addition to the metallic bismuth, bismuth oxycarbonate $Bi_2(CO_3)O_2$ is formed in the BSO3 sample.

After laser treatment of mixed colloid, the BSO1_hν and BSO2_hν samples become X-ray amorphous. In the XRD patterns of the samples two broad peaks are observed: the first one at 2θ=28° and the second low-intensity one at 2θ=48°. In the BSO3_hν sample, the metallic bismuth disappears, while the amount of bismuth oxycarbonate

$Bi_2(CO_3)O_2$ increases, and the bismuth sillenite $Bi_{12}SiO_{20}$ is also formed. Therefore, the laser treatment of mixed colloid initiates the interaction of the components and results in the formation of an interface between bismuth and silicon.

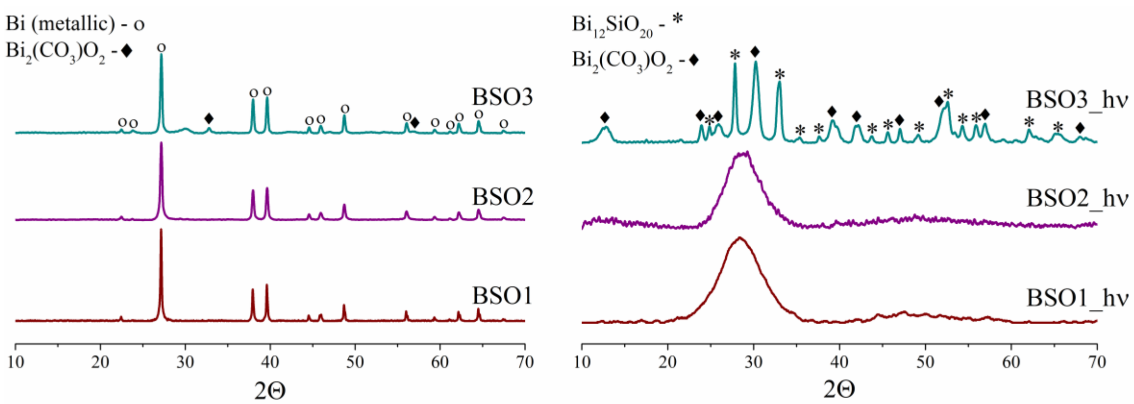

Figure 1. XRD patterns of the BSO samples

Table 1. Phase composition, specific surface area (SSA) and band gap (E_g) of the samples

Sample	**Sample composition**		**SSA, m^2/g**	**E_g, eV**	
	Phase	**%**		**Tauc**	**DASF**
BSO1	Bi	100	41	-	-
BSO1_hν	amorphous		57	**3.61 (direct)** 3.2 (undirect)	**3.62**
BSO2	Bi	100	40	-	-
BSO2_hν	amorphous		53	**3.52 (direct)** 2.9 (undirect)	**3.78**
BSO3	Bi	78	36	-	-
	$Bi_2(CO_3)O_2$	22			
BSO3_hν	$Bi_2(CO_3)O_2$	69	43	3.57 (direct) **3.0 (undirect)**	**3.15 ($Bi_{12}SiO_{20}$)** and 3.65 ($Bi_2(CO_3)O_2$)
	$Bi_{12}SiO_{20}$	31			

Figure 2 shows TEM images of the samples. The morphology of the BSO1 and BSO2 samples is similar and is represented by small particles, close to spherical, with a primary size of 20-30 nm. The laser treatment of the colloids leads to insignificant changes in the size characteristics of the particles. As a result of the treatment, the BSO1_hν and BSO2_hν samples contain both smaller particles (10 nm and less) due to fragmentation and separate large (more than 30 nm) fused particles. In general, the average particle size decreases, while the particle size distribution expands.

The BSO3 and BSO3_hν samples have a distinct morphology. The low silicon content in the samples partially stabilizes the bismuth. In addition to small spherical particles, flat lamellas, which are similar to the structures obtained by PLA of bismuth in water[26], formed in BSO3. Flat lamellas refer to the formation of oxycarbotane in the structure.

After laser treatment, the number and size of layered structures increase and needle-like structures appear; a large number of small spherical nanoparticles up to 10 nm in size are also present.

The TEM data are in accordance with the SSA data (Table 1). According to SSA data, as a result of laser treatment, the surface area of the samples increases by 1.2-1.4 times.

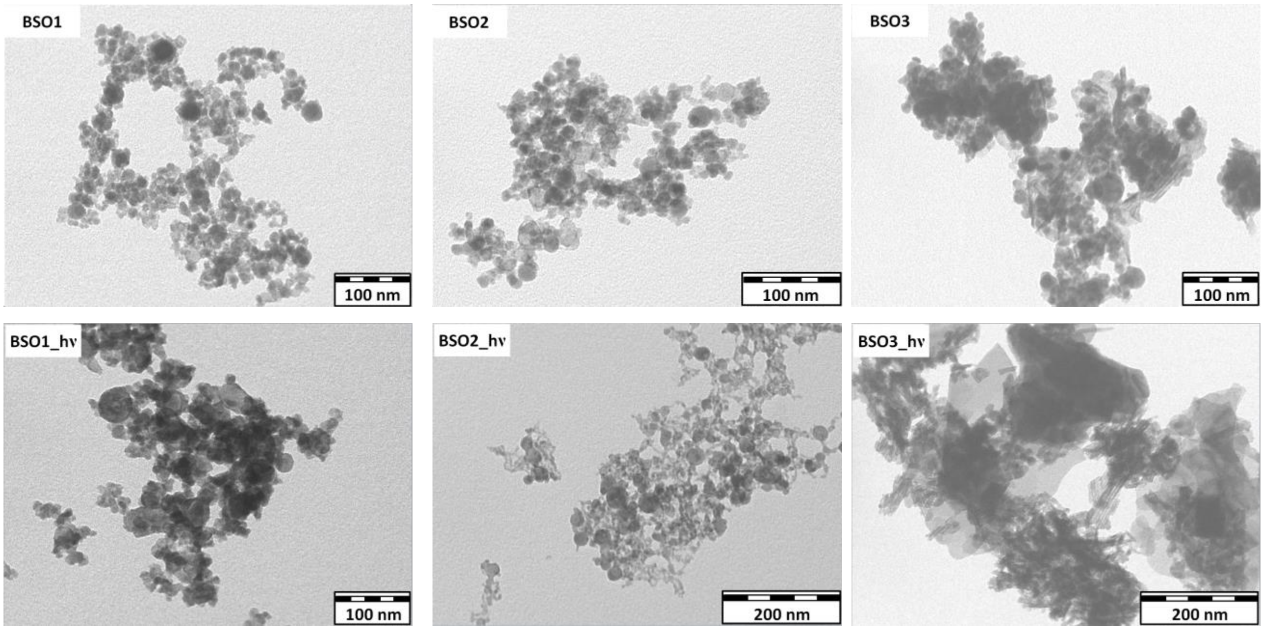

Figure 2. TEM images of the BSO samples

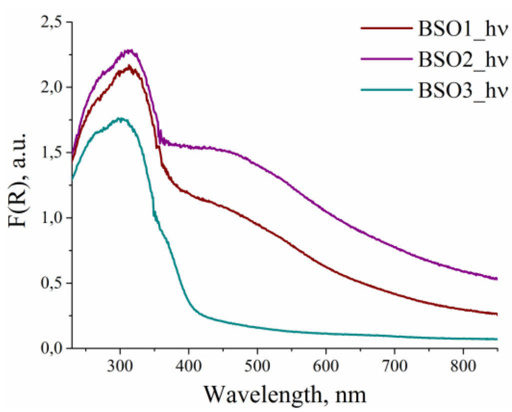

Figure 3. UV-Vis spectra of the samples after laser post-processing

Figure 3 shows UV-Vis spectra for samples obtained from the colloids after laser treatment. The samples obtained from the non-irradiated colloids are black due to the presence of the metallic bismuth and therefore absorb in the entire visible range (spectra do not shown). The BSO1_hν and BSO2_hν samples are light-toned beige and the BSO3_hν sample becomes white. The absorption spectrum of the BSO1_hν sample clearly shows the edge of the optical absorption band in the region of 310-380 nm, which corresponds to the absorption of Bi_2SiO_5[27]. The spectrum also contains additional absorption in the region of 500 nm, which can be attributed to the absorption of β-Bi_2O_3[28]. For the BSO2_hν sample, the absorption band edge is slightly shifted to longer wavelengths up to 400 nm, with the absorption band edge being correspond to both metasilicate and bismuth orthosilicate. The absorption in the region of 500 nm, possibly belonging to the absorption of β-Bi_2O_3, becomes clearer for BSO2_hν. The absorption spectrum of the BSO3_hν sample has the clear absorption band edge in the region of 400 nm, which corresponds to the absorption of the sillenite phase $Bi_{12}SiO_{20}$[29], as well as a shorter band, which may be related to bismuth oxycarbonate. Therefore, the optical spectra of the samples confirm the formation of the semiconductor structure of bismuth silicates in the samples after laser treatment.

The optical band gap for the short-wavelength absorption band edge was estimated using both the Tauc method[30] and the DASF (derivation of absorption spectrum fitting) method[31] (Table 1). For the Tauk method, the results are presented both for the case of indirect-gap transitions of the semiconductor $Bi_{12}SiO_{20}$ and direct-gap transitions for Bi_2SiO_5. DASF method does not require taking into account the type of optical transition[31]. Comparing the data obtained by the Tauc and DASF methods, one can say that the long-wavelength absorption band is determined by the direct transitions for the BSO1_hν and BSO2_hν samples, and by the indirect transition for the BSO3_hν sample.

3.2 Photocatalytic activity

Figure 4 illustrates the change in the spectra of Rhodamine B as a result of LED irradiation in the presence of the catalyst.

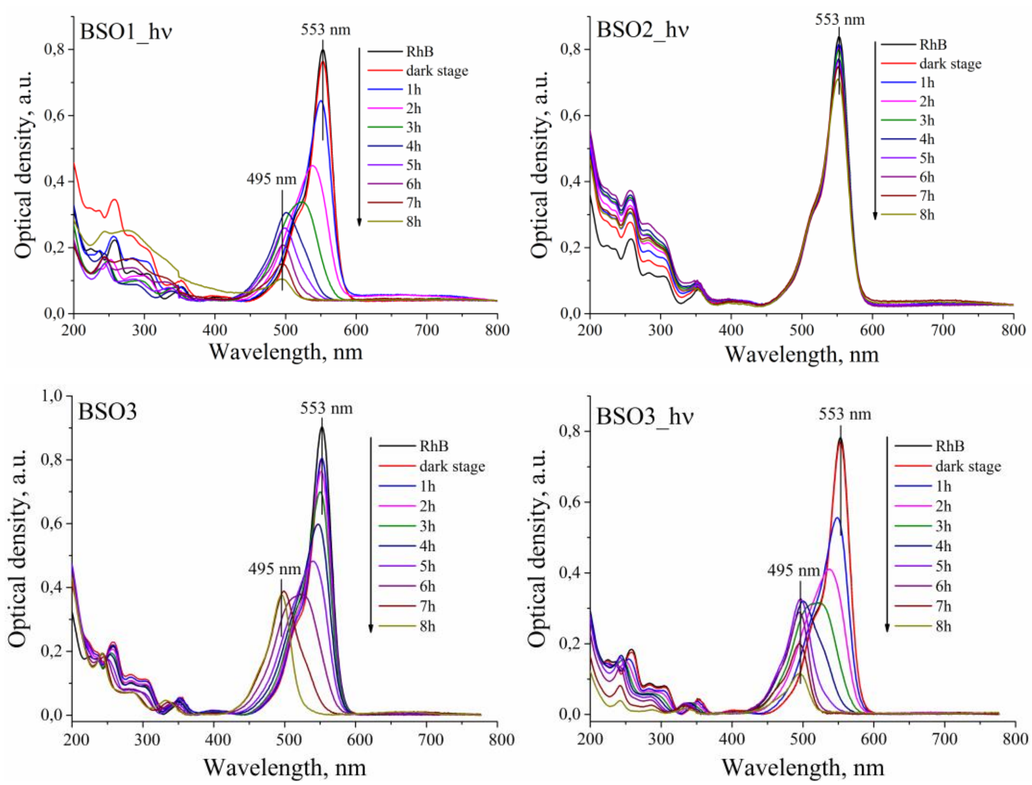

Figure 4. Changes in the absorption spectra of Rhodamine B during photocatalytic test

The BSO1 and BSO2 samples do not exhibit photocatalytic activity (the spectra do not present for brevity). This is due to the fact that samples mainly consist of metallic bismuth particles and amorphous silicon oxide. The BSO2_hν sample shows very weak activity towards Rhodamine B degradation. At the same time, the very similar BSO1_hν sample is more active. Thus, it can be assumed that the bismuth orthosilicate $Bi_4Si_3O_{12}$ is beginning to form in the BSO2_hν sample, which is the least photocatalytically active phase among the bismuth silicates.

According to the data on the photocatalytic decomposition of Rhodamine B in the presence of the BSO1_hν, BSO3, and BSO3_hν samples (figure 4), a hypsochromic shift of the absorption maximum of the dye is observed in the spectra in addition to the decrease of the optical density. This indicates the formation of intermediate products caused by N-diethylation of Rhodamine B[27]. The diethylated product absorbs at a wavelength of 495 nm and can be attributed to the absorptions of Rhodamine B 110[27]. Figure 5 shows kinetic curves of the decomposition of the initial form of the dye. The photodegradation rate constants determined using these dependences characterize exactly the process of N-diethylation of Rodamin B. The BSO1_hν and BSO3_hν samples have a high N-diethylation rate constant of 0.02-0.025 min^{-1}, while the BSO3 sample N-diethylates the dye about half as slowly. All these samples completely diethylate the initial dye of Rhodamine B.

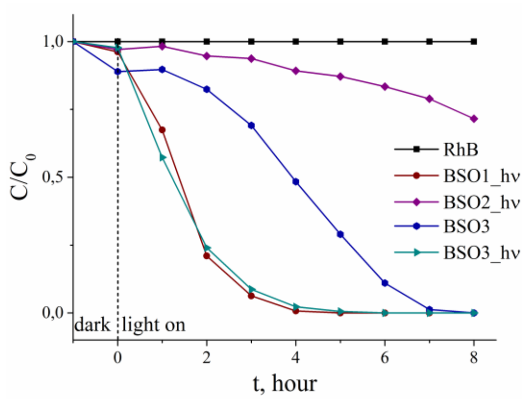

Figure 5. Kinetic curves of the photodegradation of Rhodamine B.

Under further irradiation, decomposition of diethylated product occurs. This process is more efficient for the BSO1_hν sample.

4. CONCLUSION

This work proposed the promising method for preparation of complex bismuth and silicon oxides (bismuth silicates), combining the preparation of colloids of individual components by laser ablation in water and following laser treatment of mixed colloid. It was shown that laser treatment of mixed colloid stimulates interaction between component particles and leads to formation of Si-Bi interface. Specifically, X-ray diffraction analysis showed that the samples obtained at the Bi:Si ratios of 2:1 and 4:3 are amorphous, while the sample obtained at the Bi:Si ratio of 12:1 consists of the crystalline $Bi_2(CO_3)O_2$ and $Bi_{12}SiO_{20}$ phases. Furthermore, the absorption characteristic of semiconductor oxides – bismuth silicates was indicated by absorption spectra.

The study of the photocatalytic properties of the materials showed that metasilicate and bismuth sillenite exhibit good photocatalytic activity towards the decomposition of Rhodamine B under LED irradiation, with the photodegradation processes of the dye going through the N-diethylation process.

ACKNOWLEDGEMENTS

This work was supported by Russian Science Foundation (project No. 19-73-30026).

REFERENCES

[1] Oller, I., Malato, S. and Sanchez-Perez, J. A., "Combination of Advanced Oxidation Processes and biological treatments for wastewater decontamination – A review," Sci. Total Environ. 409 (20), 4141-4166 (2011).

[2] Svetlichnyi, V. A., Tchaikovskaya, O. N., Bazyl’, O. K., Kuznetsova, R. T., Sokolova, I. V., Kopylova, T. N. and Meshalkin, Yu. P., "Photolysis of phenol and para-chlorophenol by UV laser excitation," High Energy Chem. 35(4), 258-264 (2001).

[3] Chong, M. N., Jin, B., Chow, C. W. K. and Saint, C., "Recent developments in photocatalytic water treatment technology: A review," Water Research 44 (10), 2997-3027 (2010).

[4] Low, J., Yu, J., Jaroniec, M., Wageh, S. and Al-Ghamdi, A. A., "Heterojunction Photocatalysts," Adv. Mater. 29 (20), 1601694 (2017).

[5] Wang, Q. and Domen, K., "Particulate Photocatalysts for Light-Driven Water Splitting: Mechanisms, Challenges, and Design Strategies," Chem. Rev. 120(2), 919-985 (2020).

[6] Linsebigler, A. L., Lu, G. and Yates, J. T., "Photocatalysis on TiO_2 Surfaces: Principles, Mechanisms, and Selected Results," Chem. Rev. 95(3), 735-758 (1995).

[7] Gavrilenko, E. A., Goncharova, D. A., Lapin, I. N., Gerasimova, M. A. and Svetlichnyi, V. A., "Photocatalytic activity of zinc oxide nanoparticles prepared by laser ablation in a decomposition reaction of rhodamine B," Rus. Phys. J. 63 (8), 1429-1437 (2020).
[8] Zheng, X., Fan, Y., Peng, H. and Wen, J., "S-defected In_2S_3/ZnS nanospheres for enhancing solar-light photocatalytic capacity," Colloids Surf. A 627, 127126 (2021).
[9] Bao, N., Shen, L., Takata, T. and Domen, K., "Self-templated synthesis of nanoporous CdS nanostructures for highly efficient photocatalytic hydrogen production under visible light," Chem. Mater. 20 (1), 110-117 (2008).
[10] Biryukov, A. A., Gotovtseva, E. Y., Svetlichnyi, V. A. and Gavrilenko, E. A., "Synthesis and photocatalytic properties of SiO_2/CdO/CdS nanocomposite materials," Rus. J. Appl. Chem. 87 (11), 1599-1606 (2014).
[11] Wang, C. C., Li, J. R., Lv, X. L., Zhang, Y. Q. and Guo, G., "Photocatalytic organic pollutants degradation in metal–organic frameworks," Energy Environ. Sci. 7, 2831-2867 (2014).
[12] Lee, K. M., Chin, W. L., Ngai, K. S. and Juan, J. C., "Recent developments of zinc oxide based photocatalyst in water treatment technology: A review," Water Research 88, 428-448 (2016).
[13] Al-Keisy, A., Ren, L., Zheng, T., Xu, X., Higgins, M., Hao, W. and Du, Y., "Enhancement of charge separation in ferroelectric heterogeneous photocatalyst $Bi_4(SiO_4)_3$/Bi_2SiO_5 nanostructures," Dalton Transactions 46 (44), 15582-15588 (2017).
[14] Belik, Yu., Kharlamova, T., Vodyankin, A., Svetlichnyi, V. and Vodyankina, O., "Mechanical activation for soft synthesis of bismuth silicates," Ceram. Int. 46(8), 10797-10806 (2020).
[15] Takamori, T., "The system Bi_2O_3-SiO_2," J. Am. Ceram. Soc. 73(1), 158-160 (1990).
[16] Mahmoud, H. R., "Bismuth silicate ($Bi_4Si_3O_{12}$ and Bi_2SiO_5) prepared by ultrasonic-assisted hydrothermal method as novel catalysts for biodiesel production via oleic acid esterification with methanol," Fuel 256, 115979 (2019).
[17] Karthik, K., Devi, K. S., Pinheiro, D. and Sugunan, S., "Photocatalytic activity of bismuth silicate heterostructures synthesized via surfactant mediated sol-gel method," Mater. Sci. Semicond. Process 102, 104589 (2019).
[18] Wu, Y., Chang, X., Li, M., Hei, X., Liu, C. and Zhang, X., "Studying the preparation of pure $Bi_{12}SiO_{20}$ by Pechini method with high photocatalytic performance," J. Sol-Gel Sci. Technol. 97, 311-319 (2021).
[19] Reichenberger, S., Marzun, G., Muhler, M. and Barcikowski, S., "Perspective of Surfactant-free Colloidal Nanoparticles in Heterogeneous Catalysis," CemCatChem 11, 1-31 (2019).
[20] Kibis, L. S., Stadnichenko, A. I., Svintsitskiy, D. A., Slavinskaya, E. M., Romanenko, A. V., Fedorova, E. A., Stonkus, O. A., Svetlichnyi, V. A., Fakhrutdinova, E. D., Vorokhta, M., Šmid, B., Doronkin, D. E., Marchuk, V., Grunwaldt, J. D. and Boronin, A. I., "In situ probing of Pt/TiO_2 activity in low-temperature ammonia oxidation," Cat. Sci. Technology 11(1), 250-263 (2021).
[21] Forsythe, R. C., Cox, C. P., Wilsey, M. K. and Müller, A. M., "Pulsed Laser in Liquids Made Nanomaterials for Catalysis," Chem. Rev. 121 (13), 7568-7637 (2021).
[22] Fakhrutdinova, E. D., Shabalina, A. V., Gerasimova, M. A., Nemoykina, A. L., Vodyankina, O. V. and Svetlichnyi, V. A., "Highly Defective Dark Nano Titanium Dioxide: Preparation via Pulsed Laser Ablation and Application," Materials 13(9), 2054 (2020).
[23] Amendola, V., Amans, D, Ishikawa, Y., Koshizaki, N., Scire, S., Compagnini, G., Reichenberger, S. and Barcikowski, S., "Room-Temperature Laser Synthesis in Liquid of Oxide, Metal-Oxide Core-Shells, and Doped Oxide Nanoparticles," Chem. Eur. J. 26, 9206-6242 (2020).
[24] Svetlichnyi, V. A., Belik, Y. A., Vodyankin, A. A., Fakhrutdinova, E. A. and Vodyankina, O. V., "Laser fragmentation of photocatalyst particles based on bismuth silicates," Proc. SPIE 11322, 113221D (2019).
[25] Svetlichnyi, V. A., Shabalina, A. V., Lapin, I. N., Goncharova, D. A., Kharlamova, T. S. and Stadnichenko, A. I., "Comparative Study of Magnetite Nanoparticles Obtained by Pulsed Laser Ablation in Water and Air," Appl. Surf. Sci. 467-468, 402-410 (2019).
[26] Svetlichnyi, V. A., Fakhrutdinova, E. D., Nazarova, T. S., Kulinich, S. A. and Vodyankina, O. V., "Comparative study of bismuth composites obtained via pulsed laser ablation in a liquid and in air for photocatalytic application," Solid State Phenomena 312, 172-178 (2020).
[27] Wu, Y., Li, M., Yuan, J. and Wang, X., "Synthesis and characterizations of metastable Bi_2SiO_5 powders with a synergistic effect of adsorption and photocatalysis," Appl. Phys. A 123, 543 (2017).
[28] Dou, L., Jin, X., Chen, J., Zhong, J., Li, J., Zeng, Y. and Duan, R., "One-pot solvothermal fabrication of S-scheme OVs-Bi_2O_3/Bi_2SiO_5 microsphere heterojunctions with enhanced photocatalytic performance toward decontamination of organic pollutants," Appl. Surf. Sci. 527, 146775 (2020).

[29] Li, W. Q., Wen, Z. H., Tian, S. H., Shang, L. J. and Xiong, Y., "Citric acid-assisted hydrothermal synthesis of a self-modified $Bi_2SiO_5/Bi_{12}SiO_{20}$ heterojunction for efficient photocatalytic degradation of aqueous pollutants," Catal. Sci. Technol. 8, 1051–1061 (2018).
[30] Guayaquil-Sosa, J. F., Serrano-Rosales, B., Valadés-Pelayo, P. J. and de Lasa, H., "Photocatalytic hydrogen production using mesoporous TiO_2 doped with Pt," Appl. Catal. B 211, 337-348 (2017).
[31] Souri, D. and Tahan, Z. E., "A new method for the determination of optical band gap and the nature of optical transitions in semiconductors," Appl. Phys. B 119, 273-279 (2015).